

Irradiation-induced defects in different glasses demonstrated on a metaphosphate glass

Doris Möncke and Doris Ehart

Otto-Schott-Institut für Glaschemie, Friedrich-Schiller-Universität, Jena (Germany)

The influence of the two polyvalent ions, cobalt and nickel, on the formation of irradiation-induced defects was studied in several different model glasses (silicate, borosilicate, fluoride- and phosphate glasses). In this article the defects are demonstrated on the example of the $(\text{SrPO}_3)_2$ -metaphosphate glass P100.

Sample plates of high-purity glasses, undoped and doped with 0.3 mol% CoO and NiO, were irradiated with a UV lamp and with X-rays. The subsequent defect centers, formed at ppm levels, were characterized by EPR as well as optical UV-VIS spectroscopy. Defect recovery experiments were also studied in these glasses.

The newly found optical bands and EPR signals evolving in the irradiated glass are in part characteristic for intrinsic defects. These are different types of electron centers (EC) and hole centers (HC) connected with phosphate groups. Other signals arise from extrinsic defects, which are caused by the two dopant ions. The predominant extrinsic defect stems from the photooxidation of Co^{2+} to $(\text{Co}^{2+})^+$. As an HC the latter replaces some of the intrinsic phosphate-bonded HC and dominates the optical spectra with two bands at 300 and 400 nm. In the glass P100 lamp irradiation photoionizes only Co^{2+} but not Ni^{2+} . A new optical band at 330 nm, as well as a new EPR signal at $g = 2.08$ can be seen only after X-ray irradiation. Both can be attributed to a nickel-related EC created via the photoreduction of Ni^{2+} to $(\text{Ni}^{2+})^-$. At the same time the band of the intrinsic oxygen-related HC is intensified.

Generally X-ray irradiation causes stronger irradiation-induced defects (excitation of inner electrons) than UV-lamp irradiation (selective excitation of valence electrons).

Strahlungsinduzierte Defekte in verschiedenen Gläsern dargestellt am Beispiel eines Metaphosphatglases

Der Einfluß der Dotierungen CoO und NiO auf die strahlungsinduzierte Defektbildung wurde in verschiedenen Modellgläsern (Silicat-, Borosilicat- Fluorid- und Phosphatgläsern) untersucht. In diesem Artikel werden die gebildeten Defekte exemplarisch am $(\text{SrPO}_3)_2$ -Metaphosphatglas P 100 besprochen.

Probenplättchen hochreiner undotierter und mit 0,3 Mol-% CoO- und NiO-dotierter Gläser wurden sowohl UV-Lampen als auch energiereicher Röntgenstrahlung ausgesetzt. Zur Charakterisierung der strahlungsinduzierten Defekte wurde die EPR- sowie die optische UV-VIS-Spektroskopie eingesetzt. Zusätzlich wurde in den bestrahlten Gläsern auch das Ausheilverhalten der Defekte untersucht.

Ein Teil der optischen Banden und EPR-Signale, die sich nach der Bestrahlung in den Gläsern zeigten, konnte intrinsischen Defekten, die an Phosphatgruppen auftreten und aus unterschiedlichen Elektronenzentren (EC) und Lochzentren (HC) bestehen, zugeordnet werden. Daneben wurden zusätzliche extrinsische Defekte gefunden, die auf die beiden Dotierungen zurückzuführen sind. Co^{2+} wird zu $(\text{Co}^{2+})^+$ photooxidiert. Als Lochzentrum ersetzt $(\text{Co}^{2+})^+$ einen Teil der intrinsischen phosphatgebundenen HC und dominiert die optischen Spektren mit zwei Banden bei 300 und 400 nm. Lampenbestrahlung photoionisiert im P100 nur Co^{2+} , nicht aber Ni^{2+} . Erst durch Röntgenbestrahlung tritt auch in den NiO-dotierten Gläsern eine zusätzliche Bande bei 330 nm auf. Außerdem wird ein neues EPR-Signal bei $g_1 = 2,08$ gefunden. Beide Signale entsprechen einem extrinsischen nickel-verknüpften EC. Ein Teil des Ni^{2+} wird demnach zu $(\text{Ni}^{2+})^-$ photoreduziert, während parallel die Bildung sauerstoffgebundener HC zunimmt.

Insgesamt führte Röntgenbestrahlung zu stärkeren strahlungsinduzierten Defekten (Anregung von inneren Elektronen) als UV-Lampenbestrahlung (selektive Anregung von Valenzelektronen).

1. Introduction

Radiation-induced defects in glasses require high attention due to the intensified applications of stronger lamps and lasers, working at increasingly shorter wavelengths. Solarization describes the effect of decreased trans-

mission in the UV and VIS due to color centers generated by irradiation. These color centers, or defects, evolve in ppm concentrations when the irradiation suffices to ionize the glass. The defects can be divided into negative charged electron centers (EC) and corresponding positive charged hole centers (HC) [1].

Cobalt- and nickel-doped glasses are used as optical filters. They show high transmission from 250 to

Received 15 December 2000, revised manuscript 30 April 2001.

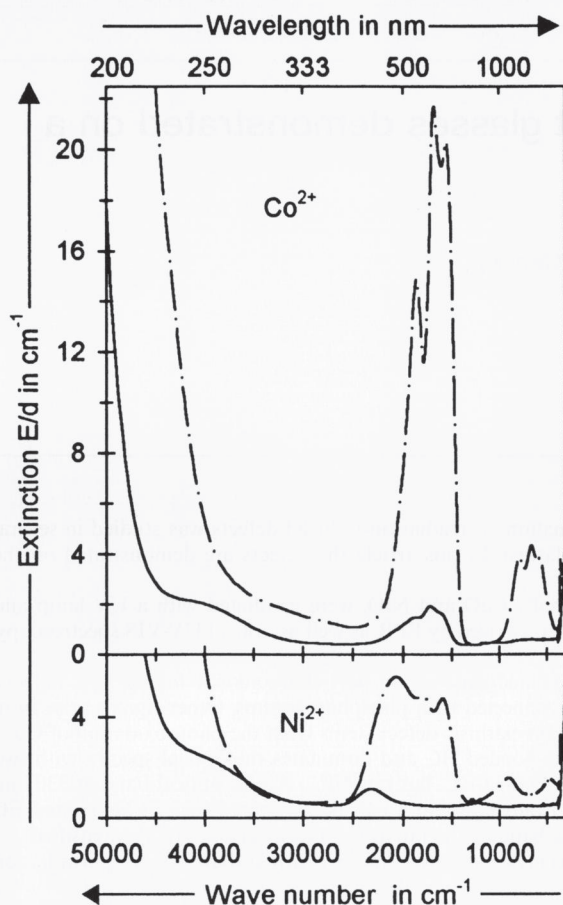


Figure 1. Optical spectra of two glasses doped with 0.3 mol% CoO and NiO; Co^{2+} (top) and Ni^{2+} (bottom), both tetrahedrally coordinated in NBS1 (---), and octahedrally coordinated in P100 (—).

400 nm. At the same time the absorption between 450 and 700 nm is very strong. Cobalt and nickel are polyvalent as well as polycoordinated ions. These ions are hardly ever seen in glasses in any other oxidation state than +2. In this state, the coordination is either tetrahedral (T_d) or octahedral (O_h) depending strongly upon the glass matrix. The differently coordinated ions show distinctive spectra and therefore different colors, leading to their use as structure indicators [2]. The typical spectra of the differently coordinated ions are shown in figure 1.

The optical basicity (A) of the glass is a measure of the electron donor power of the glass matrix [2 to 7]. A is proportional to the electron density on the oxide (-2) and can be correlated to the coordination of the Co^{2+} and Ni^{2+} ions [8]. In more acidic glasses, the ions show ionic-bonded octahedral coordination, while covalent-bonded tetrahedral coordination prevails in high basicity glasses. P100 is a metaphosphate glass with an optical basicity of $A_{\text{Pb}} = 0.47$, and thus has an intermediate position among the studied model glasses and can be classified as covalent.

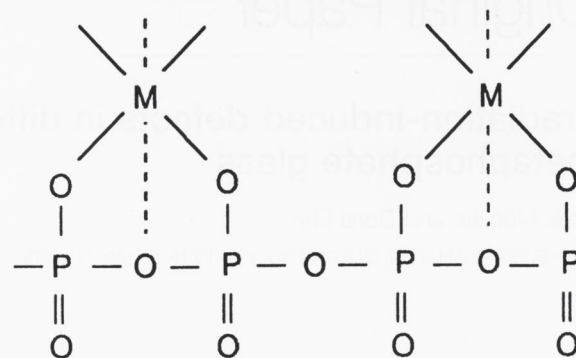


Figure 2. Schemata of the structural model of metaphosphate glasses.

Phosphate glasses possess low melting viscosities ($\eta \approx 1$ dPa s, at melting temperatures of $\approx 1200^\circ\text{C}$). The structure model of metaphosphate glasses may be described as chains of PO_4 - T_d and cations (figure 2). Due to their special optical properties, such as a high transmission in the UV, phosphate glasses are attractive candidates for application in high-performance optics and laser technology and have been melted commercially [1, 9 and 10].

Solarization by different radiation sources has already been studied in several CoO- and NiO-doped model glasses discussed in previous papers [11 and 12]. The glasses range from the acidic fluoride-phosphates FP4 and FP20 over P100 and the borosilicate glass NBS2 of medium basicity to the high basicity borosilicate and silicate glasses NBS1 and NCS (table 1). When relative weak lamp irradiation is applied, hardly any solarization is seen in any of the undoped glasses. P100 is the only undoped glass to show significant intrinsic defects. In comparison, the undoped (boro-)silicate glasses are quite stable against irradiation. However, (boro-)silicate glasses doped with CoO and NiO in tetrahedral coordination show very strong effects. This can be ascribed to the photooxidation of Co^{2+} and Ni^{2+} forming $(\text{Co}^{2+})^+$ and $(\text{Ni}^{2+})^+$ [11]. In these glasses a high basicity glass matrix stabilizes the higher oxidation states. Photooxidation of Co^{2+} is also seen in the FP glasses, in which Ni^{2+} is photoreduced to $(\text{Ni}^{2+})^-$ [12]. Nickel has a lower redox potential than cobalt and the ionic, extreme acidic FP glass matrix helps to stabilize the reduced nickel-species.

The kinetics of formation and recovery of induced defects in FP and phosphate glasses irradiated with lamps and lasers were intensively studied [9, 10, 13 to 16]. The numerous induced intrinsic defects were characterized by EPR and optical spectroscopy. A summary of the parameters is given in table 2. [9 and 16]. Based on the former results on solarization in undoped glasses, the aim of this work is to investigate in the model glass P100 the influence of the dopants NiO and CoO on the al-

Table 1. Composition (in mol%) and characteristics of the model glasses studied in this and previous papers [11 and 12]

	P100	FP20	FP4	NBS2	NBS1	NCS
	100 Sr(PO ₃) ₂	20 Sr(PO ₃) ₂ 80 { AIF ₃ MgF ₂ SrF ₂ CaF ₂	4 Sr(PO ₃) ₂ 96 { AIF ₃ MgF ₂ SrF ₂ CaF ₂	74 SiO ₂ 21 B ₂ O ₃ 4 Na ₂ O 1 Al ₂ O ₃	74 SiO ₂ 10 B ₂ O ₃ 16 Na ₂ O	74 SiO ₂ 10 CaO 16 Na ₂ O
$A_{th}^{1)}$	0.46	0.38	0.35	0.48	0.53	0.57
$A_{pb}^{2)}$	0.47	0.45	0.34			
ΣFe in ppm	8	10	10	5	5	5
Fe ³⁺ in ppm	5	6	6			
T_g in °C	510	490	440	440	550	530
n_e	1.56	1.50	1.43	1.47	1.51	1.52
ρ in g/cm ³	3.15	3.51	3.46	2.18	2.45	2.49
coordination	O _h	O _h	O _h	O _h	T _d	T _d
color ³⁾	{ Co violet Ni amber	violet amber	violet amber	violet yellow-green	blue violet	blue brown
solarization	less pronounced	less pronounced	less pronounced	less pronounced	very strong	very strong

¹⁾ Theoretical optical basicity according to Duffy [3 to 6].

²⁾ Optical basicity values experimentally determined via the Pb²⁺ indicator ion as found by Seeber [7].

³⁾ NiO and CoO were doped in concentrations of 0.3 mol%, respectively.

ready characterized defects and also the formation of any new defect centers.

2. Experimental procedures

Table 1 displays the compositions and optical basicities of several model glasses studied. The phosphate glasses were melted at 1350 °C in an electric furnace in SiO₂ crucibles in 100 g batches. They were cooled in graphite molds from 550 °C to room temperature with a cooling rate of about 30 K/h. The glasses were melted as undoped base glasses, doped with 0.3 mol% CoO and NiO, respectively, and with 0.15 mol% both CoO and NiO. Only high-purity reagents were used for melting so that the iron content of the glasses could be kept as low as 5 to 10 ppm.

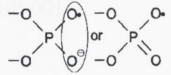
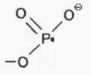
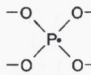
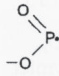
Polished plates (10 x 20 x 2) mm³ were irradiated with an HgXe broad band lamp and similar samples 1 mm thick were irradiated with X-rays. The 1 kW HgXe lamp works in a sunsimulator from ORIEL and continuously emits a wide spectrum from the UV to the NIR. The spectral power density of the lamp was about 1500 W/m² in that part of the spectrum between 230 to 280 nm, which causes most of the solarization damage. The samples were placed at a 10 cm distance from the radiation source and irradiated up to 100 h to ensure that defect formation reached a saturation level.

For X-ray irradiation, the sample plates were subjected to a copper-cathode radiation of 10 kW (50 kV, 200 mA) at a distance of 80 cm. In this case irradiation lasted 16 h.

Experiments of thermal recovery were performed afterwards. The irradiated samples were heated for 1 h before the optical spectra were taken. The temperatures were raised in steps from 50 to 150 °C until the transformation temperature of the glass was reached. Quantitative and qualitative changes in the optical spectra of the various defect centers at different temperatures helped in the task of band separation and classification of the spectral data.

UV-VIS-NIR spectra were used to characterize the glasses and to observe the irradiation-induced effects. A double-beam spectrophotometer (UV-3102 PC, Shimadzu) was employed, recording the extinction $E = \lg(I_0/I)$ with an error <1%. The extinction was later standardized on a nominal path length (d) of 1 cm. The induced extinction ($\Delta E/d$), or change of optical density caused by the irradiation, is used to describe the defects. The bands of the evolving electron centers are usually found near the UV edge. The dopants absorb strongly in this range, complicating the evaluation of the optical bands. Therefore a second, independent analytical method, the Electron Paramagnetic Resonance spectroscopy (EPR), was applied. For comparison the glasses were also analyzed with the addition of the spin-standard dpph (1,1-diphenyl-2-picrylhydrazyl). All spectra displayed within one series were taken from samples of the same dimension and as such could be standardized. Although Co²⁺ and Ni²⁺ compounds are known to be successfully investigated by EPR, Co²⁺ and Ni²⁺ in glass give no visible EPR signals and could only be detected at extremely low temperatures [17 and 18]. As no signals seem to arise in glasses from Co²⁺ and Ni²⁺, EPR spectroscopy permits the detection of para-

Table 2. Paramagnetic constants and optical absorption of radiation-induced defects in phosphate glasses [14 to 16]

defect type	EPR parameters ⁴⁾	optical absorption ⁵⁾		W' in eV	structure ⁶⁾
		λ in nm	E' in eV		
POHC (HC)	$W = 1$ mT	540	2.30 ± 0.02	0.50	
	$A_{\text{iso}} = (4.0 \pm 0.3)$ mT	430	2.89 ± 0.04	1.00	
	$g_{\text{m}} = 2.008 \pm 0.003$	325	3.82 ± 0.04	1.12	
PO3 (EC)	$W = 10$ mT $A_{\text{iso}} = (86 \pm 2)$ mT $g_{\text{m}} = 2.064 \pm 0.005$	210	5.90 ± 0.06	1.00	
PO4 (EC)	$W = 9$ mT $A_{\text{iso}} = (126 \pm 2)$ mT $g_{\text{m}} = 2.142 \pm 0.008$	240	5.12 ± 0.06	1.00	
PO2 (EC ⁴⁾)	$W = 7$ mT $A_{\text{iso}} = (27 \pm 2)$ mT $g_{\text{m}} = 2.006 \pm 0.003$	265	4.68 ± 0.08	1.00	
OHC (HC)	$W = 7$ mT $g = 2.014 \pm 0.001$	290	4.28 ± 0.06	1.00	oxygen-related center of unknown structure
(Co ²⁺) ⁺⁷⁾ (HC)	no signal	300 400	4.13 ± 0.01 3.10 ± 0.03	1.24 1.20	
(Ni ²⁺) ⁻⁷⁾ (EC)	$W = 6$ mT $g = 2.1$	330	3.75 ± 0.03	1.00	Ni ²⁺ -stabilized EC

⁴⁾ W = the half amplitude width of the line; A_{iso} = (isotope) hyperfine splitting due to ³¹P, the distance (in mT) between two lines; g_{m} = the middle value between g values of both lines of a doublet: $g_{\text{mid}} = (g_1 + g_2)/2$.

⁵⁾ λ = wavelength of the band maximum (error ± 5 nm); E' = energy of the band maximum; W' = half amplitude width of the band (error $\pm (0.03-0.07)$ eV).

⁶⁾ O = oxygen ion; P = phosphorus ion; \ominus = negative charge; \bullet = paramagnetic electron.

⁷⁾ Parameters of the extrinsic defects observed in this study.

magnetic EC and HC in glasses at room temperature without interferences from the two dopants [11]. The EPR spectrometer used (ESP 300 E, Bruker) worked with a frequency band of $\nu \approx 9.78$ GHz. The resolved Gaussian bands of the induced optical spectra were correlated with defect centers detected by EPR and optical spectra of thermal recovery measurements. Band separation of the diverse spectra was accomplished on the computer with customary auxiliary software.

3. Results and discussion

Figure 1 shows the optical spectra of the differently coordinated ions. Due to the different symmetries and thus $d \rightarrow d$ transition probabilities the intensities of the bands of the tetrahedrally coordinated ions are about 100 times higher than those of the octahedrally coordinated ions. As nickel strongly favors the octahedral over the tetrahedral coordination even the high basicity NBS1 glass displays a mixed spectrum of both coordinated Ni²⁺ ions [19]. In P100 cobalt and nickel show the typical spectra of the octahedral coordinations (figure 1).

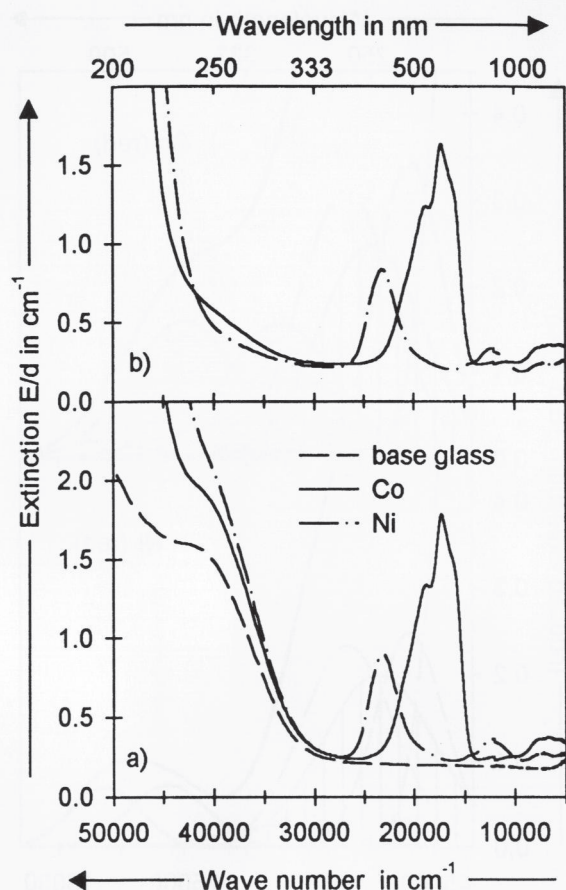
The optical spectra of the differently doped P100 glasses can be seen in figures 3a and b. The shoulder at 250 nm is caused by the charge-transfer (CT) transition

of Fe³⁺. Assuming a molar extinction coefficient of $0.18 \text{ ppm}^{-1} \text{ cm}^{-1}$, Fe³⁺ is present at a level of 5 ppm in the glasses melted under normal conditions [14]. Minor unsimilarities of the melting conditions lead to fluctuating Fe²⁺/Fe³⁺ ratios. In this case raw materials with slightly more reducing qualities were used for two glasses further referred to as reduced-melted samples. The absorption edge of the spectra below 250 nm results from the CT transition of the two dopants Co²⁺ and Ni²⁺.

Solarization in glasses doped simultaneously with CoO and NiO can be explained by the combination of the defects found in the monodoped glasses. Further discussion will therefore concentrate on the undoped- and monodoped-melted glasses.

3.1 Irradiation by lamp

The undoped model glasses, with the exception of P100, were relatively stable in regard to solarization. P100 shows the typical defects arising in phosphate glasses even after weak lamp irradiation. Form and magnitude of intrinsic defects in undoped phosphate glasses have been characterized by both spectral methods. Table 2 lists the defects parameter as found by Ebeling [15 and 16], while figure 4 gives an example of the typical EPR



Figures 3a and b. Optical spectra of preirradiated P100 undoped and doped with 0.3 mol% CoO and NiO; a) normal melts (5 ppm Fe^{3+} /3 ppm Fe^{2+}), b) reduced melts (8 ppm Fe^{2+}).

signals found in irradiated phosphate glasses. The optical spectra are characterized in the region of longer wavelengths by three bands which are ascribed to the POHC. The bands of the different phosphate-bonded EC (PEC) are found at shorter wavelengths near the UV. Band separation of the defects found in the undoped glasses was based on the parameters as stated in table 2.

The optical spectra of the lamp-induced defects can be seen in figures 5 and 6. Comparison of the defects in the differently doped glasses show that the $\text{Fe}^{2+}/\text{Fe}^{3+}$ ratio has a strong influence on form and magnitude of the spectra, especially in the region of shorter wavelengths. The high extinction coefficient of the CT band from the $(\text{Fe}^{2+})^+$ formed by photooxidation and the correspondingly formed EC are responsible for the high absorption below 300 nm. The extent of the iron photooxidation depends upon the initial amount of Fe^{2+} in the glasses and thus the induced loss of transmission is stronger in the reduced-melted glasses [14].

The POHC signals are very similar in the undoped and the NiO-doped glasses. The spectra are characteristically different for CoO-doped glasses. The induced optical spectra can be fitted with two added bands at 300

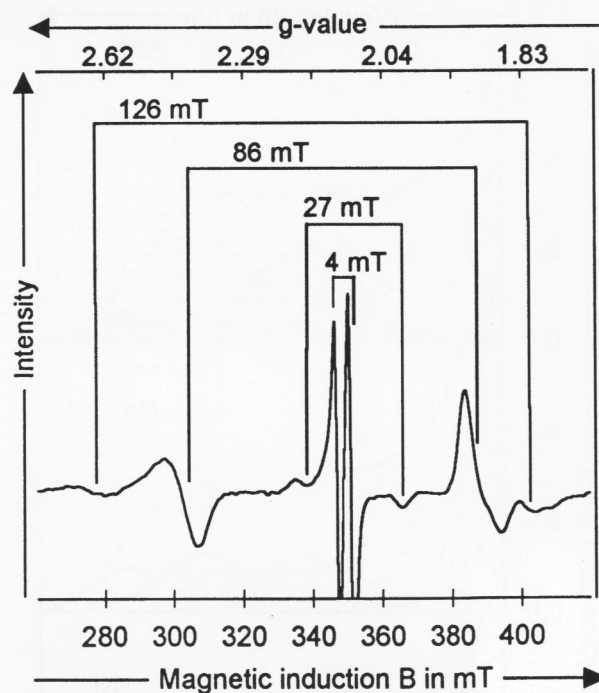


Figure 4. Example of EPR signals found in undoped X-ray irradiated phosphate glasses according to [9 and 16]; the A_{iso} values of the intrinsic defects are labeled as stated in table 2: PO_4EC (126 mT), PO_3EC (86 mT), PO_2EC (27 mT), POHC (4 mT).

and 500 nm, and lowered POHC bands. The optical spectra of octahedral Co^{3+} is described in the literature with two analogous bands between 300 and 500 nm [20]. The two newly found bands confirm the interpretation of a photooxidation of Co^{2+} forming $(\text{Co}^{2+})^+$ [11 and 12]. $(\text{Co}^{2+})^+$ as HC partially replaces some of the intrinsic POHC, whereas $(\text{Fe}^{2+})^+$ is formed only in addition to the intrinsic HC.

The EPR spectra of the glasses irradiated by lamp are displayed in figure 7. The spectra of the undoped and the NiO-doped glasses are in good agreement. The main differences can be seen in the PEC signals, which are notably more pronounced for the NiO-doped glass. This is easily explained, as the NiO-doped glass analyzed is one of the more reduced-melted ones whereas the base glass is a normal-melted one. The photooxidation of iron results in the parallel formation of PEC and thus causes the higher magnitude of the PEC signals. The small variations in the POHC signals do not significantly exceed the error margins.

However, the EPR spectra for the CoO-doped glass show a sharp decline of the POHC signals without changes in the intensities of the PEC signals. The photooxidized $(\text{Co}^{2+})^+\text{HC}$ replaces some POHC, while the amount of intrinsic PEC stays the same regardless of the dopant (figure 7).

The P100 glass matrix has a less stabilizing effect on the photooxidized dopant than the glass matrix of the

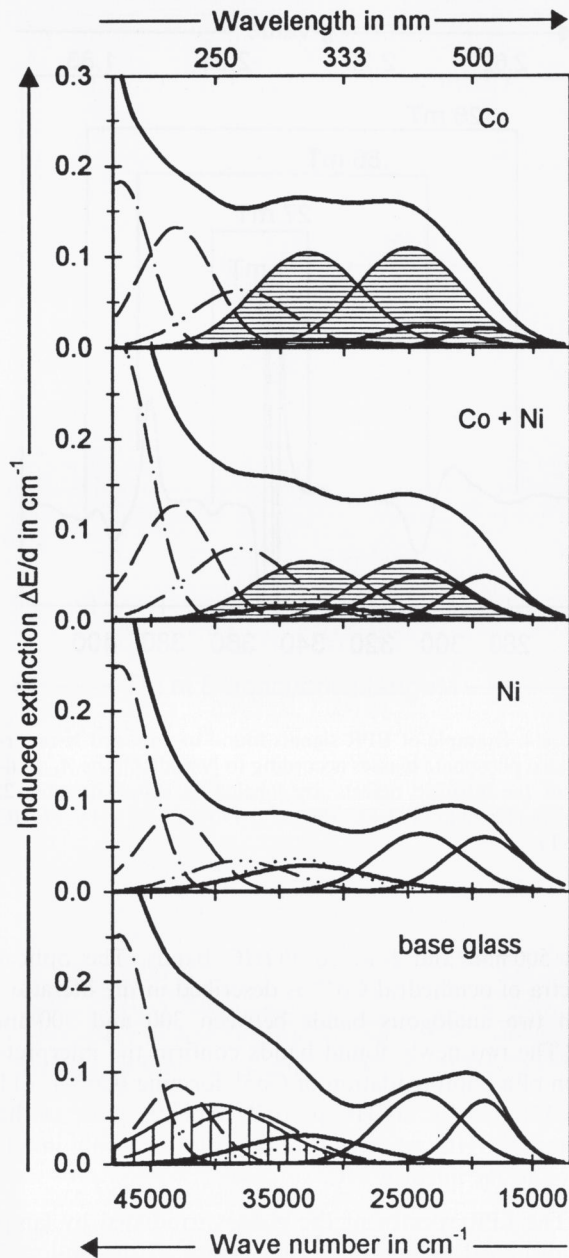


Figure 5. Induced optical spectra including band simulation of XeHg-lamp irradiated normal-melted P100: PO₂EC (---), PO₄EC (---), PO₃EC (---), POHC (—), OHC (····), (Co²⁺)⁺HC (≡), (Fe²⁺)⁺HC (|||) < 0.5 ppm.

high basicity (boro-)silicates. Only cobalt with a higher oxidation potential than nickel is photooxidized.

A more detailed observation of the induced defects shows that the (Co²⁺)⁺ bands in the induced optical spectra of the normal-melted glass doped only with CoO is twice as high as in the glass doped with CoO as well as NiO. The glass doped with both ions has only half the CoO content of the monodoped glass. The glass doped with CoO and NiO has a lower concentration of (Co²⁺)⁺HC than the CoO-doped glass and therefore a higher concentration of POHC and OHC. These how-

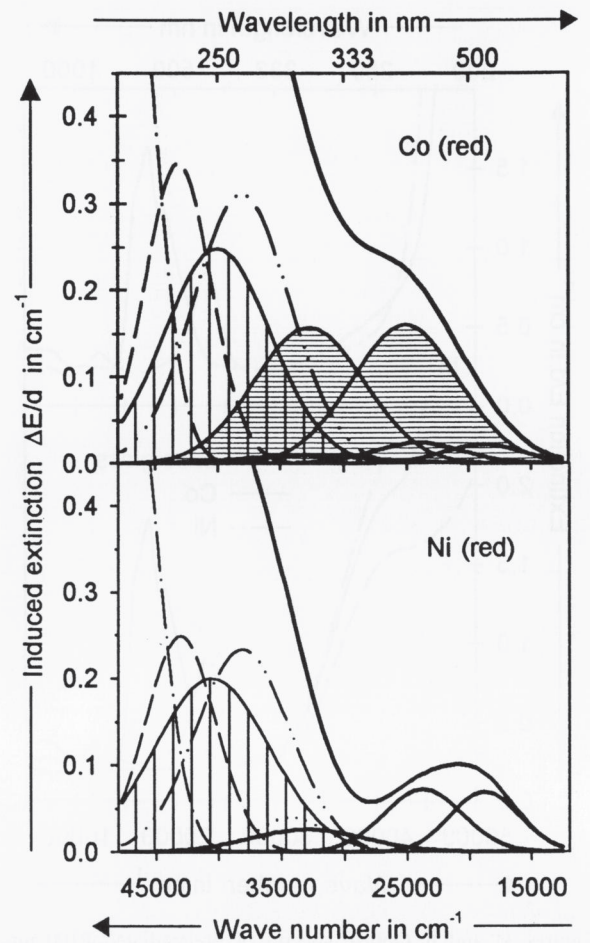


Figure 6. Induced optical spectra including band simulation of XeHg-lamp irradiated reduced-melted P100 (red): PO₂EC (---), PO₄EC (---), PO₃EC (---), POHC (—), OHC (····), (Co²⁺)⁺HC (≡), (Fe²⁺)⁺HC (|||) ≈ 1 ppm.

ever are of lower magnitudes in the glass doped with CoO and NiO than in the NiO-doped glass. The EPR spectra are in good agreement with the findings of the optical spectra.

Further the (Co²⁺)⁺ bands in the induced optical spectra of the reduced-melted CoO-doped glass are increased by as much as 30 % in relation to the normal-melted glass. No changes are found within the POHC signals. Comparison of the two reduced-melted glasses show that the formation of (Fe²⁺)⁺ and PEC is higher in the CoO- than in the NiO-doped glass. It seems that the combination of Fe²⁺ and Co²⁺ enhances the photooxidation of each of the two ions.

3.2 Irradiation by X-rays

High-energy X-ray irradiation will excite all kinds of possible effects in the glasses, while lamp irradiation excites only a small number of well defined defects. There-

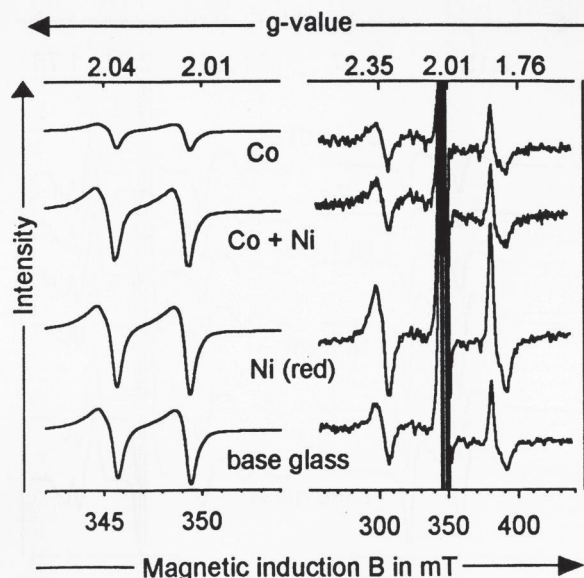


Figure 7. EPR spectra of doped and undoped XeHg-lamp irradiated P100, dpph-standardized: section displaying the POHC signals (left); magnified PEC signals (right); (red) = reduced-melted glasses.

fore extrapolation from X-ray to long-term UV-lamp solarization is not advisable. The results of X-ray irradiation should be discussed nevertheless, as this method leads to new defects and the intensities of the defects known from lamp irradiation were several magnitudes higher.

The optical spectra (figures 8 and 9) after X-ray irradiation have a very similar form to those after lamp irradiation, merely the intensity of the defects is increased by a factor of 50 for the undoped and NiO-doped and of 100 for the CoO-doped glasses.

However, the form of the spectrum of the NiO-doped glass shows a new feature in regard to the spectra after lamp irradiation. Band separation gives for the NiO-doped glasses only a good fit when an additional band at 350 nm is added. This band has been connected before to the photoreduction of Ni^{2+} to $(\text{Ni}^{2+})^-$ [12].

In CoO-doped glasses X-ray irradiation leads once again to the photooxidation of Co^{2+} to $(\text{Co}^{2+})^+$. The induced optical spectra of the CoO-doped glasses show that most POHC are replaced by $(\text{Co}^{2+})^+\text{HC}$ and that additional intrinsic PEC are formed, just as found after lamp irradiation.

The EPR spectra (figure 10) resemble the spectra taken after lamp irradiation. The strong decrease of the POHC signal is once more apparent for the CoO-doped glass. The magnified spectra of the PEC signals are very similar for all glasses, with the exception of one new defect found in all the NiO-doped glasses. A small signal evolves on the low field side of the POHC signal at $g = 2.1$.

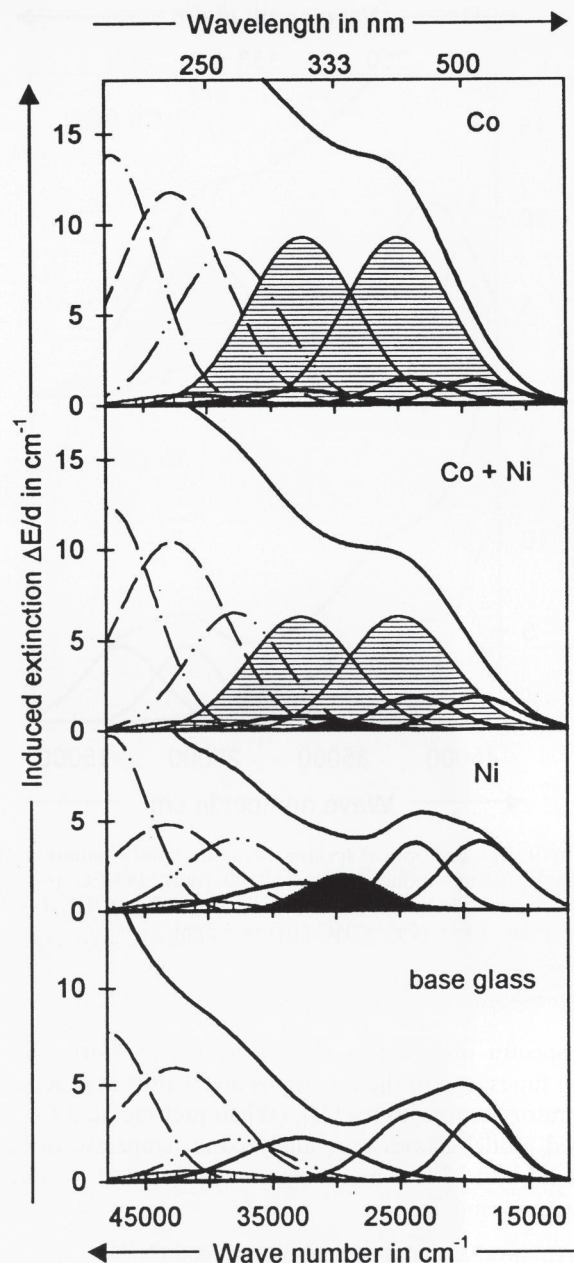


Figure 8. Induced optical spectra including band simulation of X-ray irradiated normal-melted P100: PO_2EC (\cdots), PO_4EC ($- - -$), PO_3EC ($- \cdot - \cdot -$), $(\text{Ni}^{2+})^-\text{EC}$ (\blacksquare), POHC (---), $(\text{Co}^{2+})^+\text{HC}$ (\equiv), $(\text{Fe}^{2+})^+\text{HC}$ (\llcorner) ≈ 3 ppm.

Although Co^{2+} and Ni^{2+} do not seem to be visible at room temperature in EPR spectra of glasses, Ni^{2+} as d^9 or inverse d^1 -species exhibits its own signal. One explanation for the absence of a Co^{2+} and Ni^{2+} signal might arise from a tetragonal or trigonal distortion of their complexes, leading to low-lying excited states instead of the normally found degeneracy of octahedral complexes. The low-lying excited state results from minimal quenching of orbital motion and gives rise to exceedingly short relaxation times and large spectral anisotropies. The latter causes the particularly smear out of

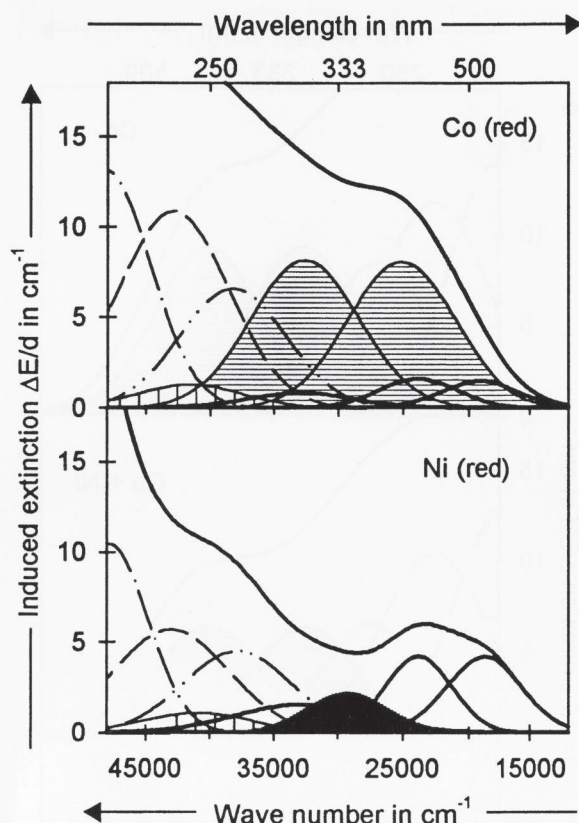


Figure 9. Induced optical spectra including band simulation of X-ray irradiated reduced-melted P100 (red): PO_2EC (---), PO_4EC (- -), PO_3EC (- · -), $(\text{Ni}^{2+})^- \text{EC}$ (■), POHC (—), $(\text{Co}^{2+})^+ \text{HC}$ (≡), $(\text{Fe}^{2+})^+ \text{HC}$ (|||) ≈ 5 ppm.

the spectra observed in glasses, while the short relaxation times lead to the enormous line widths at practical laboratory temperatures [21]. (When preirradiated CoO-doped model glasses were analyzed at temperatures between 4 and 77 K a broad signal was found at g values between 4 and 7).

Anyhow, a signal of a photoreduced $(\text{Ni}^{2+})^-$ species has been found in the acidic FP glasses [12]. Compared to the two irradiation-induced signals in the FP glasses which were attributed to $(\text{Ni}^{2+})^-$, only one signal is found in the P100 glass. The optical spectra do however support the evolution of a photoreduced $(\text{Ni}^{2+})^-$ species just as in the FP glasses. The different form of the EPR data might be satisfactorily explained with the high sensitivity of this method of analysis for the bonding characteristics of a paramagnetic ion. In such a way a nickel-related signal with a g value of ≈ 2.1 has been reported in the literature [22]. This signal seemed to arise rather from Ni^{2+} stabilizing a reduced ligand than from a fully reduced Ni^+ species. A model of the two differently reduced nickel-complexes is shown in figure 11.

The high basicity of the P100 glass compared to FP glass may influence the bonding characteristics within the newly formed nickel-related EC. Dopants are by no means isolated ions within the glass matrix. NiO_6 octa-

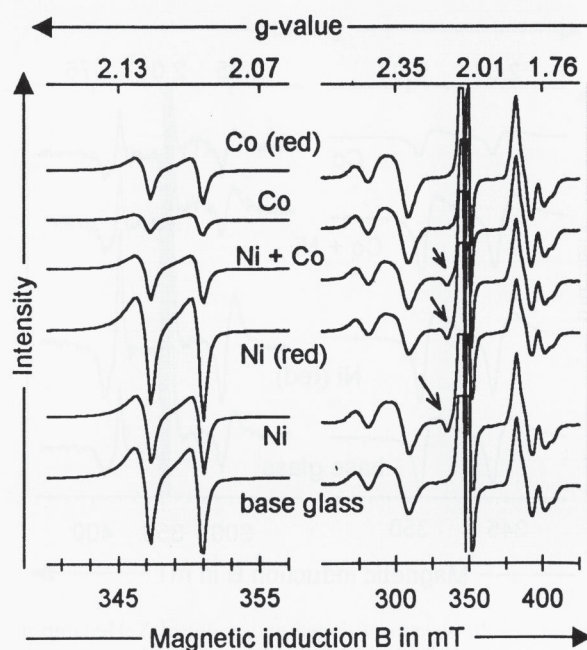
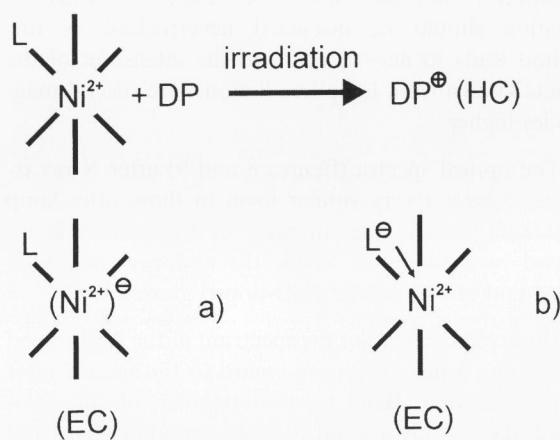


Figure 10. EPR spectra of doped and undoped X-ray irradiated P100, dpph-standardized: section displaying the POHC signals (left); magnified EC signals (right); the nickel-associated signal is pointed out by arrows; (red) = reduced-melted glasses.



Figures 11a and b. Different forms of radiation-induced defects based on Ni^{2+} in doped glasses; a) 'wholly' reduced $(\text{Ni}^{2+})^-$ ion as found in the acidic FP glasses, b) nickel-associated EC where a reduced ligand (L) is stabilized by Ni^{2+} as found in the more covalent P100 (DP = defect precursor, source of the electron $^{\ominus}$).

hedrals are present in the first sphere within phosphate glasses. The bonds are predominantly ionic in the relative acidic FP glasses and photoreduction of the Ni^{2+} leads to a more ionic $(\text{Ni}^{2+})^-$. In the more covalent MP glass with its higher basicity the photoreduced $(\text{Ni}^{2+})^-$ has still a higher Ni^{2+} character. The electron surplus center is rather spread over the adjoining ligands. The true form of the EC complex may probably be found

somewhere between the two displayed forms. EPR analysis is more sensitive to slight changes in the bonding characteristics of the paramagnetic ion than the optical spectroscopy.

Hence strong X-ray irradiation leads in P100 to the photoionization of Ni^{2+} and forms via photoreduction a Ni^{2+} -related EC, which shows only one EPR signal at $g \approx 2.1$. And, contrary to the acidic FP glasses, weak lamp irradiation does not cause any photoreduction of Ni^{2+} or other nickel-related defects in the covalent P100. On the other hand a photooxidation of Ni^{2+} is found in the high basicity silicate and borosilicate model glasses.

As seen before, a difference between the normal- and the reduced-melted NiO-doped glasses arises as seen before from the different $\text{Fe}^{2+}/\text{Fe}^{3+}$ ratios. The magnitude of the formed $(\text{Fe}^{2+})^+$ band is almost twice as strong in the reduced-melted than in the normal-melted glasses. The simultaneous photooxidation of Co^{2+} and Fe^{2+} enhances the overall photooxidation to a lesser extent than observed after lamp irradiation.

3.3 Recovery experiments

The irradiated samples showed different rates of recovery when left in the dark at room temperature for two months. While the undoped and NiO-doped glasses could recover as much as half of the induced extinction after X-ray irradiation, the CoO-doped glasses only showed small recovery effects.

Thermal recovery experiments were routinely performed on irradiated samples. Soft heating of the samples gave more information for the task of band separation and classification of the defect centers. Besides the photooxidized iron, normally all irradiation-induced defects recover wholly before the temperature reaches T_g . Instead of the expected ongoing decline of the induced absorption, lamp-irradiated CoO-doped glasses displayed a distinct increase of absorption after heating to 200°C. Band simulation of the induced optical spectra in figures 12a to c show that POHC transform to $(\text{Co}^{2+})^+\text{HC}$ in the CoO-doped glasses. This conversion is observed to a lesser extent even at room temperature. Figure 12b displays the small conversion that has already taken place after months in which the sample was stored in the dark at room temperature. Heating the sample for 1 h to 200°C converses the rest (figure 12c). The final amount of $(\text{Co}^{2+})^+$ seems to be independent of the initial Co^{2+} concentration. Both the glasses doped with CoO and NiO and the glass doped only with CoO show very similar spectra with similar $(\text{Co}^{2+})^+$ concentrations. The EPR spectra taken at this point show a decline of the POHC but so far no changes in the PEC signals (figure 13).

No such conversion was observed during the annealing process in any glasses except those doped with

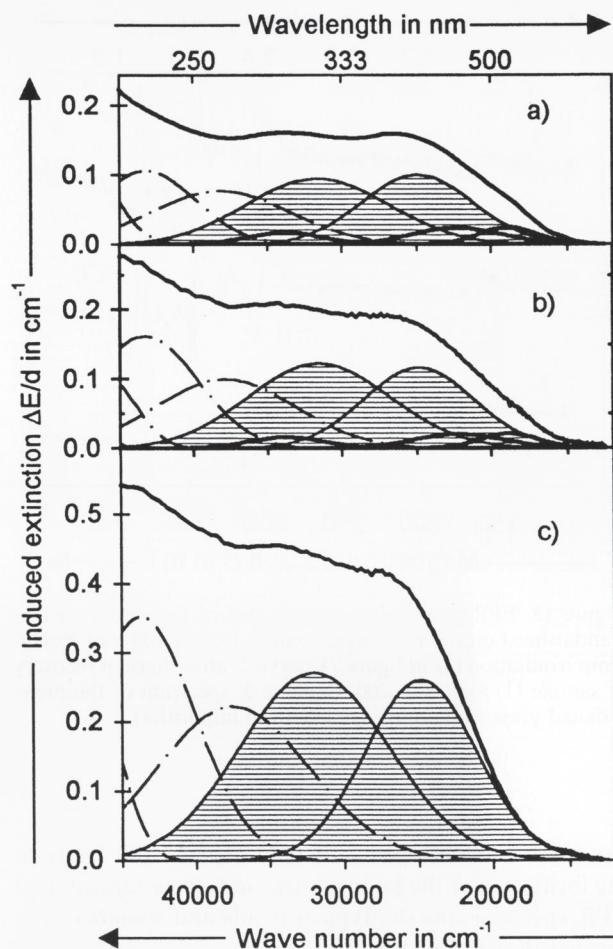


Figure 12a to c. Induced optical spectra, including band separation, of XeHg-lamp irradiated CoO-doped P100 after: a) XeHg-lamp irradiation, b) storage of this irradiated sample for three months at room temperature in the dark, c) thermal treatment of this stored sample for 1 h at 200°C; PEC (---), POHC (—), $(\text{Co}^{2+})^+\text{HC}$ (≡).

CoO. In none of the samples irradiated by X-rays did this conversion show, not even in the CoO-doped samples in which the initial defects exceed those found after lamp irradiation by a factor of 50 to 100. However, as before the undoped and NiO-doped samples recovered more easily than the CoO-doped samples and they recovered fully when the temperatures reached 250°C. The CoO-containing glasses had to be heated up to 400°C to produce similar results. It is also interesting that in the CoO-doped glasses even the band of the photooxidized $(\text{Fe}^{2+})^+$ disappears after heating to 400°C.

4. Conclusion

The irradiation source had a great influence on solarization. As expected, high-energy X-rays induce intense defects. The magnitude of these defects were 50 to 100 times greater than those after lamp irradiation. Lamp

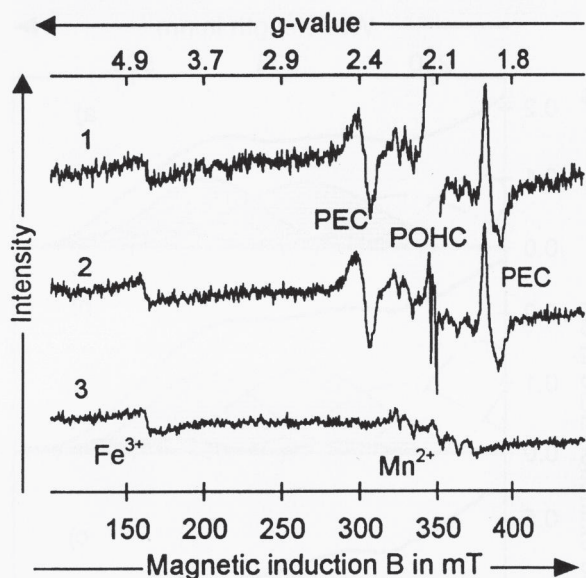


Figure 13. EPR spectra of a normal-melted CoO-doped P100, standardized on the Fe^{3+} signal; curve 1: after 100 h of XeHg-lamp irradiation (as in figure 7), curve 2: after thermal recovery of sample (1) for 1 h at 200°C , curve 3: spectrum of the pre-irradiated glass (signals arise solely from impurities).

irradiation of undoped and NiO-doped P100 leads to the formation of the known intrinsic defects. Optical and EPR spectra show the typical bands and signals of the formed POHC and PEC.

Defects in the CoO-doped glasses differ significantly from the undoped and NiO-doped glasses. Co^{2+} is easily photooxidized to $(\text{Co}^{2+})^+$. The optical spectra are characterized by two bands of similar magnitude at 300 and 450 nm. $(\text{Co}^{2+})^+$ is more easily formed than intrinsic POHC. $(\text{Co}^{2+})^+$ not only replaces some of the POHC but is also formed in excess, leading to a parallel increase in the known PEC.

Recovery experiments showed that thermal treatment led in lamp-irradiated glasses below 200°C to a transformation of POHC into $(\text{Co}^{2+})^+\text{HC}$ before any actual recovery began at higher temperatures. This effect was not found in the X-ray irradiated glasses.

Ni^{2+} is less easily photoionized than Co^{2+} . Compared to the undoped base glass, no significant increase of solarization is observed after lamp irradiation. Contrary to Co^{2+} , where X-ray irradiation only enhances the photooxidation, Ni^{2+} is photoreduced to $(\text{Ni}^{2+})^-$ by strong X-ray irradiation. The optical spectra show an additional band at 350 nm, which compares well with the literature data of Ni^+ . The EPR spectra also reveal an additional signal at $g = 2.1$. It seems that the optical basicity of P100 is not acidic enough to favor the photoreduction to $(\text{Ni}^{2+})^-$ in the same way as the ionic FP glasses, where even lamp irradiation photoreduced Ni^{2+} to $(\text{Ni}^{2+})^-$ [12]. Strong X-ray irradiation nevertheless leads in the more covalent P100 via photoreduction to

an Ni^{2+} -related EC, which shows only one EPR signal at $g \approx 2.1$. EPR analysis is more sensitive to slightly different bonding characteristics of the paramagnetic ion than optical spectroscopy and thus a different signal is found for the different nickel-related EC in the FP glasses and P100.

Comparison of the defects in the differently doped glasses show that the $\text{Fe}^{2+}/\text{Fe}^{3+}$ ratio also has a strong influence on the form and magnitude of the induced spectra. The high extinction coefficient of the CT band of $(\text{Fe}^{2+})^+$, formed by photooxidation, and the correspondingly formed EC are responsible for the high absorption below 300 nm. The simultaneous photooxidation of Co^{2+} and Fe^{2+} enhances the overall photooxidation, especially after irradiation by lamp.

5. References

- [1] Ehrdt, D.; Seeber, W.: Glass for high performance optics and laser technology. *J. Non-Cryst. Sol.* **129** (1991) p. 19–30.
- [2] Weyl, W. A.: Coloured glasses. Sheffield: Society of Glass Technology, 1951.
- [3] Duffy, J. A.: A common optical basicity scale for oxide and fluoride glasses. *J. Non-Cryst. Solids*. **109** (1989) p. 35–39.
- [4] Baucke F. G. K., Duffy J. A.: Oxidation states of metal ions in glass melts. *Phys. Chem. Glasses* **35** (1994) no. 1, p. 17–21.
- [5] Duffy J. A.: Redox equilibria in glass. *J. Non-Cryst. Solids* **196** (1996) p. 45–50.
- [6] Duffy J. A.: Charge transfer spectra of metal ions in glass. *Phys. Chem. Glasses* no. **38** (1997) no. 6, p. 289–292.
- [7] Seeber, W.: Kombination experimenteller und theoretischer Methoden der Absorptions- und Lumineszenzspektroskopie zur Entwicklung amorpher Materialien für Optik und Optoelektronik – Am Beispiel von Fluoridphosphatgläsern. Universität Jena, Habilitation thesis 1995.
- [8] Paul A.; Douglas R. W.: Optical absorption of divalent cobalt in binary alkali borate glasses and its relation to the basicity of glass. *Phys. Chem. Glasses* **9** (1968) no. 1, p. 21–26.
- [9] Ehrdt, D.; Natura, U.; Ebeling, P. et al.: Formation and healing of UV radiation defects in phosphate and fluoride phosphate glasses with high UV transmission. In: Proc. XVIII International Congress on Glass, San Francisco, CA (USA) 1998. Session C10, p. 1–6. (Available on CD-ROM from Am. Ceram. Soc.)
- [10] Ehrdt, D.; Leister, M.; Matthai, A.: Redox behaviour in glass forming melts. *Molten Salt Forum* **5–6** (1998) p. 547–554.
- [11] Möncke, D.; Ehrdt, D.: Radiation defects in CoO and NiO doped glasses of different structure. In: Proc. 5th Conf. European Society of Glass Science and Technology (ESG), Prague 1999. Vol. B4, p. 49–56. (Available on CD-ROM from Czech Glass Society.)
- [12] Möncke, D.; Ehrdt, D.: Radiation-induced defects in CoO- and NiO-doped fluoride-phosphate glasses. *Glastech. Ber. Glass Sci. Technol.* **74** (2001) no. 3, p. 65–73.
- [13] Natura, U.; Ehrdt, D.: Formation of radiation defects in silicate and borosilicate glasses caused by UV lamp and excimer laser radiation. *Glastech. Ber. Glass Sci. Technol.* **72** (1999) no. 9, p. 295–301.
- [14] Ehrdt, D.; Ebeling, P.; Natura, U.: UV transmission and radiation induced defects in phosphate and fluoride-phosphate glasses. *J. Non-Cryst. Solids* **263 & 264** (2000) p. 240–250.

- [15] Ebeling, P.; Ehrh, D.; Friedrich, M.: Study of radiation-induced defects in fluoride-phosphate glasses by means of optical absorption and EPR spectroscopy. *Glastech. Ber. Glass Sci. Technol.* **73** (2000) no. 5, p. 156–162.
- [16] Ebeling, P.: Strahlungsinduzierte Defekte in Phosphatgläsern. Universität Jena, PhD. thesis 2000.
- [17] Gan, F.; Deng, H.; Liu, H.: Paramagnetic resonance study on transition metal ions in phosphate, fluoridephosphate and fluoride glasses. Pt. 2: Co^{2+} and Ni^{2+} . *J. Non-Cryst. Sol.* **52** (1982) p. 143–149.
- [18] Pilbrow, J. R.: Transition ion electron paramagnetic resonance. Oxford: Clarendon, 1990. p. 327–331.
- [19] Bates, T.: Ligand field theory and absorption spectra of transition-metal ions in glasses. In: Mackenzie, J. D.: Modern aspects of the vitreous state. Vol. 2. London: Butterworths, 1962. p. 195–255.
- [20] Linard, M.; Weigel, M.: Lichtabsorption von Mono- und Diacido-amminen des dreiwertigen Kobalts mit Fettsäureresten. *Z. anorg. Allg. Chem.* **264** (1951) p. 321–335.
- [21] Griscom, D. L.: Electron spin resonance in glasses. *J. Non-Cryst. Sol.* **40** (1980) p. 211–272.
- [22] Bowmaker, G. A.; Boyd P. D.; Campbell, G. K. et al.: Spectroelectrochemical studies of Ni(I) complexes: One-electron reduction of nickel(II) complexes of dithiocarbamate and phosphine ligands $[\text{Ni}(\text{R}_2\text{NCS}_2)_x(\text{Ph}_2\text{PCH}_2\text{CH}_2\text{PPh}_2)_{2-x}]^{2-x}$ ($x = 0,1,2$). *Inorg. Chem.* **21** (1982) p. 1152–1159.

■ 0701P003

Address of the authors:

D. Möncke, D. Ehrh
Otto-Schott-Institut für Glaschemie
Friedrich-Schiller-Universität Jena
Fraunhofer Straße 6
D-07743 Jena